Developmental Biology 328 (2009) 13–23

Contents lists available at ScienceDirect

Developmental Biology

journal homepage: www.elsevier.com/developmentalbiology

Twisted gastrulation limits apoptosis in the distal region of the mandibular arch in mice

BreAnne MacKenzie [a], Ryan Wolff [b], Nick Lowe [b], Charles J. Billington Jr [a,c], Ashley Peterson [a], Brian Schmidt [a], Daniel Graf [d], Mina Mina [e], Rajaram Gopalakrishnan [f], Anna Petryk [a,g,*]

[a] Department of Pediatrics, University of Minnesota, Minneapolis, MN 55455-0356, USA
[b] School of Dentistry, University of Minnesota, Minneapolis, MN 55455-0356, USA
[c] Medical Scientist Training Program, University of Minnesota, Minneapolis, MN 55455-0356, USA
[d] Institute of Immunology, Biomedical Sciences Research Center 'Al Fleming', 16672 Vari, Greece
[e] Department of Pediatric Dentistry, University of Connecticut Health Center, Farmington, CT 06032-1956, USA
[f] Diagnostic/Biological Sciences, School of Dentistry, University of Minnesota, Minneapolis, MN 55455-0356, USA
[g] Department of Genetics, Cell Biology and Development, Minneapolis, MN 55455-0356, USA

ARTICLE INFO

Article history:
Received for publication 13 August 2008
Revised 3 December 2008
Accepted 31 December 2008
Available online 20 January 2009

Keywords:
Twisted gastrulation
BMP
Agnathia
Micrognathia
Neural crest
Branchial arch
Apoptosis
Smad

ABSTRACT

The mandibular arch (BA1) is critical for craniofacial development. The distal region of BA1, which gives rise to most of the mandible, is dependent upon an optimal level of bone morphogenetic protein (BMP) signaling. BMP activity is modulated in the extracellular space by BMP-binding proteins such as Twisted gastrulation (TWSG1). *Twsg1*$^{-/-}$ mice have a spectrum of craniofacial phenotypes, including mandibular defects that range from micrognathia to agnathia. At E9.5, the distal region of the mutant BA1 was prematurely and variably fused with loss of distal markers *eHand* and *Msx1*. Expression of proximal markers *Fgf8* and *Barx1* was expanded across the fused BA1. The expression of *Bmp4* and *Msx2* was preserved in the distal region, but shifted ventrally. While wild type embryos showed a gradient of BMP signaling with higher activity in the distal region of BA1, this gradient was disrupted and shifted ventrally in the mutants. Thus, loss of TWSG1 results in disruption of the BMP4 gradient at the level of signaling activity as well as *mRNA* expression. Altered distribution of BMP signaling leads to a shift in gene expression and increase in apoptosis. The extent of apoptosis may account for the variable degree of mandibular defects in *Twsg1* mutants.

Introduction

The first (mandibular) branchial arch (BA1) is critical for craniofacial development. Human syndromes that result from defective development of derivatives of BA1, with or without associated malformations, are collectively referred to as the first arch syndrome and may manifest as defects of the ears, eyes, mandible, and palate (Moss and James, 1984). BA1 bifurcates into maxillary and mandibular prominences, the latter contributing to the lower jaw (Cerny et al., 2004; Depew et al., 2002). Various degrees of underdevelopment of the mandible are observed in human syndromes. The milder form, micrognathia (small mandible), occurs in about 1 in 4000 births worldwide (Chung and Myrianthopoulos, 1975) and is a common component of human craniofacial syndromes (Dixon et al., 2007; Suri et al., 2006). The most extreme form of mandibular arch hypoplasia is agnathia, in which the lower jaw fails to develop. This is a much less common manifestation usually leading to in utero or perinatal mortality (Schiffer et al., 2002).

The mandibular arch emerges from the lateral wall of the pharynx and becomes visible in mouse embryos around E9.0 as symmetrical prominences (Thomas et al., 1998). Expansion of BA1 occurs through robust proliferation of neural crest cell-derived mesenchyme, which pushes the prominences medially (Nanci, 2003; Senders et al., 2003). At E9.5, opposing midline epithelia come in close contact, but disruption of the midline epithelium does not occur until E10.5, allowing confluence of the mesenchyme across the midline. Midline fusion is completed by E11.0 (Chai et al., 1997). Two functional regions can be distinguished along the proximo-distal axis of BA1: the proximal (lateral) region that is dependent mainly on Fibroblast growth factor 8 (FGF8) signaling and the distal (medial) region that is regulated by bone morphogenetic proteins (BMPs) (Ferguson et al., 2000; Mina et al., 2002; Thomas et al., 1998; Tucker and Sharpe, 2004). Normal development of the mandibular arch requires the proper balance between signaling pathways to offset their predominant trophic (FGF8) versus apoptotic (BMP) effects (Stottmann et al., 2001). In addition, the level, location, and timing of BMP signaling have profound

* Corresponding author. University of Minnesota, 13-124 PWB, MMC 8404, 516 Delaware Street, SE, Minneapolis, MN 55455, USA. Fax: +1 612 626 5262.
E-mail address: petry005@umn.edu (A. Petryk).

0012-1606/$ – see front matter © 2009 Elsevier Inc. All rights reserved.
doi:10.1016/j.ydbio.2008.12.041

effects on gene expression and cell survival within the developing BA1. This is particularly relevant for the development of the distal region which makes a major contribution to the overall growth of the mandible and has been referred to as the "leading edge" of the growing mandibular arch (McGonnell et al., 1998; Mina et al., 2002; Thomas et al., 1998).

Both excessive and reduced BMP signaling may adversely affect BA1 development (Ko et al., 2007; Liu et al., 2005; Solloway and Robertson, 1999). For example, mutant mice with a simultaneous deletion of BMP antagonists Chordin (CHRD) and Noggin (NOG) have hypoplastic BA1s, which is thought to be due to excessive BMP signaling, repression of *Fgf8* expression, and increased cell death (Stottmann et al., 2001). Reduction in BMP signaling, for example due to deletion of *Bmp4* in the mandibular ectoderm (Liu et al., 2005), or inactivation of *Smad4* in the neural crest (Ko et al., 2007), also leads to underdevelopment of BA1. At earlier stages, when BA1 is composed of undifferentiated mesenchyme, ectopic BMPs promote apoptosis, but at later stages BMPs promote chondrogenesis (Ekanayake and Hall, 1997; Mina et al., 2002; Wang et al., 1999). BMP4 is able to induce expression of both *Msx1* and *Msx2* in the distal mesenchyme (Tucker et al., 1998a; Vainio et al., 1993). The pro-apoptotic effect of BMPs is thought to be mediated mainly through *Msx2*, while *Msx1* may mediate a proliferative effect (Marazzi et al., 1997; Mina et al., 1995). Both genes are sensitive to different levels of BMP signaling (Liu et al., 2005).

Given the significance of BMP levels, it is important to understand how BMP signaling is regulated during BA1 morphogenesis. *Twisted gastrulation (Twsg1* in mice and humans or *tsg* in *Drosophila)* gene product is a secreted protein, which has been shown to either antagonize or promote BMP activity depending on the species, developmental timing, the organ being studied, and also its interactions with other proteins such as CHRD (Larrain et al., 2001; Nosaka et al., 2003; Oelgeschlager et al., 2003; Petryk et al., 2005; Ross et al., 2001; Wills et al., 2006). TWSG1 binds to several BMPs, including BMP2, BMP4, and BMP7. We have previously reported that TWSG1 is critical for craniofacial development (Petryk et al., 2004). Deficiency of TWSG1, particularly in C57BL/6 background, results in a spectrum of craniofacial phenotypes, including mandibular defects that range from micrognathia (Melnick et al., 2006) to agnathia. While forebrain defects and rostral truncations observed in these mice are largely due to reduced *Shh* and *Fgf8* expression, the mechanism of deficient mandibular development is not entirely understood. Here we show that in the absence of TWSG1, the BA1 region is prematurely fused, mispatterned and showing a significant increase in apoptosis as early as E9.5. Furthermore, both the expression of BMP target genes and the distribution of BMP signaling is altered, indicating that the BA1 defects are likely due to changes in BMP signaling. An increase in apoptosis results in subsequent loss of BA1 derivatives. The variable extent of apoptosis likely accounts for both the variable loss of BA1 derivatives and the spectrum of micrognathic/agnathic phenotypes.

Materials and methods

Embryo harvest and genotyping

Generation and genotyping of *Twsg1*$^{-/-}$ mice in C57BL/6 background were previously described (Petryk et al., 2004). Timed matings were set up between *Twsg1*$^{+/-}$ mice to obtain wild type and homozygous mutant littermates. Presence of a spermatic plug was considered embryonic day E0.5. Heterozygous embryos carrying *LacZ* reporter gene replacing exon 2 and most of exon 3 of *Twsg1* gene (Gazzerro et al., 2006) were used to study localization of *Twsg1* in BA1. Use and care of the mice in this study was approved by the University of Minnesota Institutional Animal Care and Use Committee.

Histology and skeletal preparation

The embryos were fixed in 4% paraformaldehyde, embedded in paraffin by standard methods and sectioned at 5–7 μm (Petryk et al., 2004). The skeletons of wild type and *Twsg1*$^{-/-}$ neonates were stained with alizarin red as described (Hogan et al., 1994).

Whole mount LacZ staining

Embryos were harvested from pregnant females at E9.5–E11.5. The embryos were washed twice in cold PBS, and fixed for 5–10 min in freshly prepared cold fixative solution (PBS containing 0.01% Na deoxycholate, 0.02% NP40, 2% formaldehyde, 0.2% glutaraldehyde). Embryos were washed 3 times in cold PBS/2 mM MgCl2 before being placed in the staining solution (0.1 M Phosphate buffer pH 7.3, 2 mM MgCl2, 0.01% Na deoxycholate, 0.02% NP40, 5 mM K3Fe(CN)6, 5 mM K4Fe(CN)6, 1 mg/ml X-Gal). Staining was performed overnight or longer at room temperature in the dark. The reaction was stopped by three washes in PBS. The embryos were post-fixed in 1% paraformaldehyde and stored in PBT at 4 °C until analysis.

In situ hybridization

Whole mount RNA in situ hybridization was performed using standard methods (Sasaki and Hogan, 1993). *Msx1* (MacKenzie et al., 1991), *Msx2* (MacKenzie et al., 1992), *Barx1* (Tissier-Seta et al., 1995), *Fgf8* (Crossley and Martin, 1995), *Bmp4* (Winnier et al., 1995), *Nog* (McMahon et al., 1998), and *eHand* (Cserjesi et al., 1995) probes have been previously described. At least three wild type and three mutant embryos were analyzed using each probe. To examine how deficiency of TWSG1 affects proximo-distal marker expression in BA1, we compared the expression of distal and proximal markers in wild type and mutant embryos with midline fusion at E9.5 and some at E10.5.

Immunohistochemistry and TUNEL assay for apoptosis

Immunohistochemistry was performed as previously published (Melnick et al., 2006). TWSG1 protein was detected by incubating the paraffin-embedded sections with monoclonal anti-mouse TSG antibody (R and D Systems) at 1:100 dilution for 2 h at 23 °C and then overnight at 4 °C, followed by incubation with goat anti-rat antibody Alexa Fluor 488 (Invitrogen) at 1:100 dilution for 2 h at 23 °C.

Immunostaining for pSMAD1/5 was performed on cryosections. The embryos were fixed overnight at 4 °C in 4% paraformaldehyde, washed in cryoprotectant (10% sucrose, 20% sucrose, and 1:1 solution of 20% sucrose and TissueTek for 1 h at 55 °C). The embryos were then embedded in Tissue-Tek O.C.T. compound (Electron Microscopy Sciences) and sectioned at 12–14 μm. The primary antibody (monoclonal anti-phospho-SMAD1/5 antibody, Cell Signaling) was incubated at 1:100 dilution for 3 h at room temperature and then overnight at 4 °C. The secondary antibody (Alexa Fluor 488 goat anti-rabbit IgG, Molecular Probes) was incubated at 1:200 dilution at room temperature for 3 h.

The DeadEnd Fluorometric TUNEL assay (Promega) was performed on paraffin-embedded sections according to manufacturer's instructions to detect apoptosis in BA1. The sections were counterstained with VECTASHIELD Mounting Medium with DAPI (Vector Labs) and viewed under the Zeiss Axioplan 2 microscope.

Quantification of apoptosis and statistical analysis

The BA1 sections from the TUNEL assay were divided into three equal sections along the proximo-distal axis (using Photoshop software) from images taken with the Zeiss Axioplan 2 microscope (left proximal, distal, and right proximal). The area of each section was

outlined within each box (Figs. 7F, G) and apoptotic cells were counted at 200× in each section per area (apoptotic index) in 3 *Twsg1*$^{-/-}$ and 11 wild type embryos. Data are expressed as the mean ± s.d. of up to 4 sections per embryo. Statistical differences were determined by ANOVA, followed by a Tukey–Kramer multiple comparison test. Significance was determined at $p<0.01$.

Results

Twsg1 gene expression and protein localization in BA1

Heterozygous embryos carrying *LacZ* reporter gene in the *Twsg1* locus were used to study *Twsg1* expression. At E9.5, the reporter gene was expressed throughout BA1, in both distal and proximal regions (Figs. 1A, B). At E10.5, a slight gradient of expression could be seen with predominance in the distal region (Figs. 1C, D). By E11.5, the reporter gene was expressed in a pattern that became restricted toward the oral epithelium and proximal arch (Figs. 1E, F). TWSG1 protein was distributed in a similar fashion, initially uniformly throughout the mesenchyme of the mandibular arch at E9.5 (Figs. 1J, K), but decreasing toward the proximal region by E10.5 (Figs. 1L, M). By E11.5, TWSG1 protein distribution shifted toward the proximal region of BA1 (Figs. 1N, O). TWSG1 protein localized to the cell membranes (Figs. 1G–I).

Derivatives of BA1, but not BA2 are missing or underdeveloped in Twsg1$^{-/-}$ *mice*

We have previously reported a spectrum of external craniofacial phenotypes at birth, which range from midline defects to more extensive loss of head structures (Petryk et al., 2004). In this paper we focus on characterization of branchial arch derivatives. The main skeletal derivative of BA1 is Meckel's cartilage, around which the mandible forms. In agnathic *Twsg1*$^{-/-}$ newborns, the mandible, and therefore all mandibular teeth, were absent (Figs. 2D–F). In micrognathic mutants, the mandibular bones were smaller and fused in the midline (Fig. 3B′) compared to the wild type mandibular bones (Fig. 3A′). BA1 gives rise not only to the mandible, but also the ossicles of the middle ear (malleus and incus), bones of the lateral skull, as well as soft tissues, including the anterior two-thirds of the tongue. Accordingly, in addition to jaw defects other BA1 derivatives were either missing or deformed in *Twsg1* knockouts (Figs. 2D–F) compared to wild type mice (Figs. 2A–C). The anterior two-thirds of the tongue that are specifically derived from BA1 were missing in *Twsg1*$^{-/-}$ mice (Fig. 2D). Both nasal and oral cavities appeared rudimentary. The oral cavity was discontinuous with the pharynx, which was also hypoplastic (Fig. 2D). We have previously reported that the morphogenesis of another BA1 derivative, the submandibular salivary gland (SMG), is abnormal in *Twsg1* mutants and that SMG phenotypes correlate with the external craniofacial phenotype, ranging from normal to agenesis/aplasia (Melnick et al., 2006). The maxilla was also affected, although to a lesser degree than the mandible perhaps due to different embryonic origin of the upper jaw (Cerny et al., 2004; Lee et al., 2004). Although the maxillary incisors were missing in *Twsg1*$^{-/-}$ mice, the maxillary molars were preserved (Fig. 2F). Mutants with severe craniofacial defects had palatal shelf hypoplasia and cleft palate (not shown). The malleus, which is derived from the proximal region of BA1 (Fig. 3A), was variably affected depending on the severity of the external craniofacial phenotype (Figs. 3B–D).

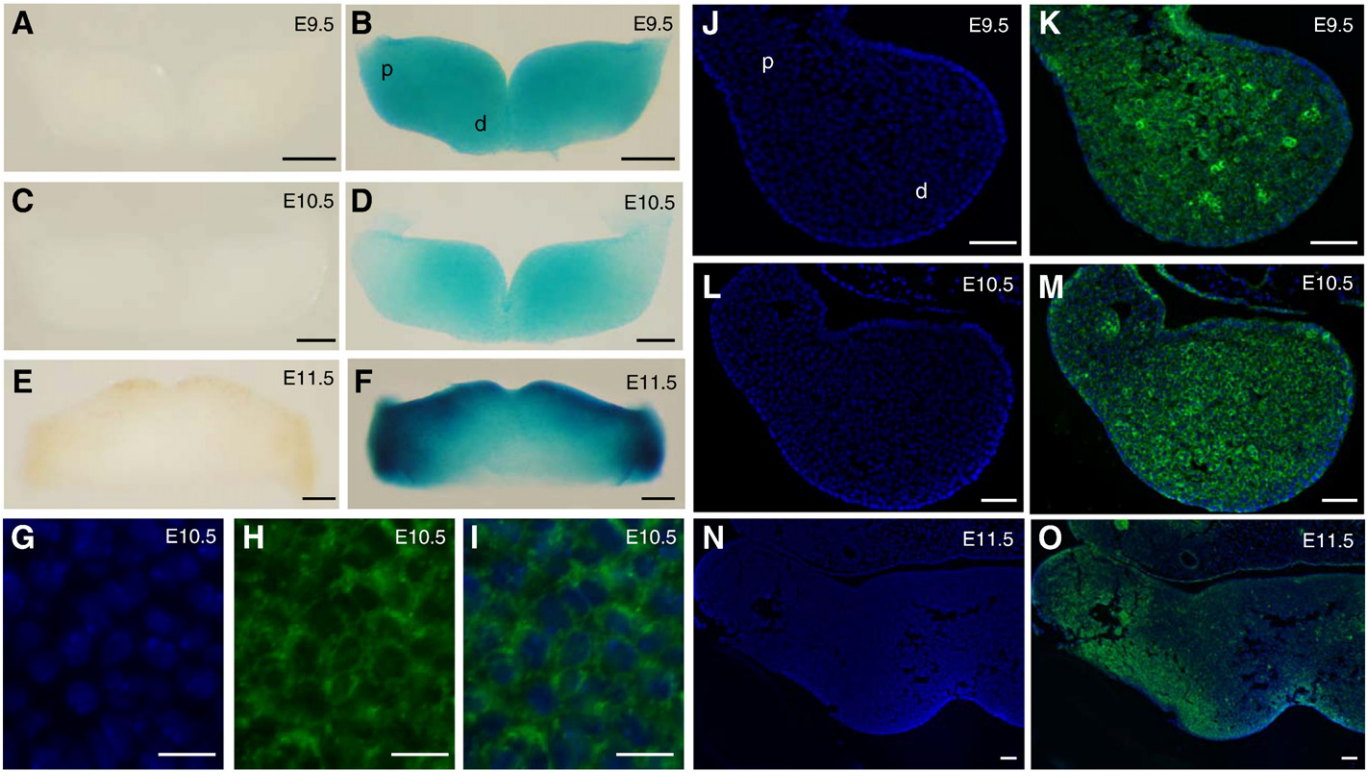

Fig. 1. *Twsg1* gene expression and protein localization in the mandibular component of BA1. (A–F) Whole mount LacZ staining of heterozygous embryos carrying *LacZ* reporter gene in the *Twsg1* locus. (A) Negative control at E9.5. (B) *LacZ* reporter gene is expressed throughout the mandibular arch at E9.5, in both distal and proximal regions. (C) Negative control at E10.5. (D) Gradient of the *LacZ* reporter gene expression at E10.5 with predominance in the distal region. (E) Negative control at E11.5. (F) The reporter gene is expressed in a pattern that is restricted toward the oral epithelium and proximal arch at E11.5. (G–O) TWSG1 protein localization by fluorescent immunostaining (right arch is shown). (G) DAPI, higher magnification of the image shown in M, (H) TWSG1 protein, (I) Overlay of DAPI and immunostaining for TWSG1 showing localization to the cell membranes, (J) DAPI, (K) Overlay of DAPI and TWSG1 immunostaining showing uniform distribution of TWSG1 throughout the mesenchyme of the mandibular arch at E9.5, (L) DAPI, (M) Overlay of DAPI and TWSG1 at E10.5 showing a gradient of distribution of TWSG1, (N) DAPI, (O) Overlay of DAPI and TWSG1 at E11.5 showing a shift in TWSG1 protein distribution toward the proximal BA1. Sections G–O are transverse sections; d, distal; p, proximal. Scale bar: 200 μm in A–F, 10 μm in G–I, 50 μm in J–O.

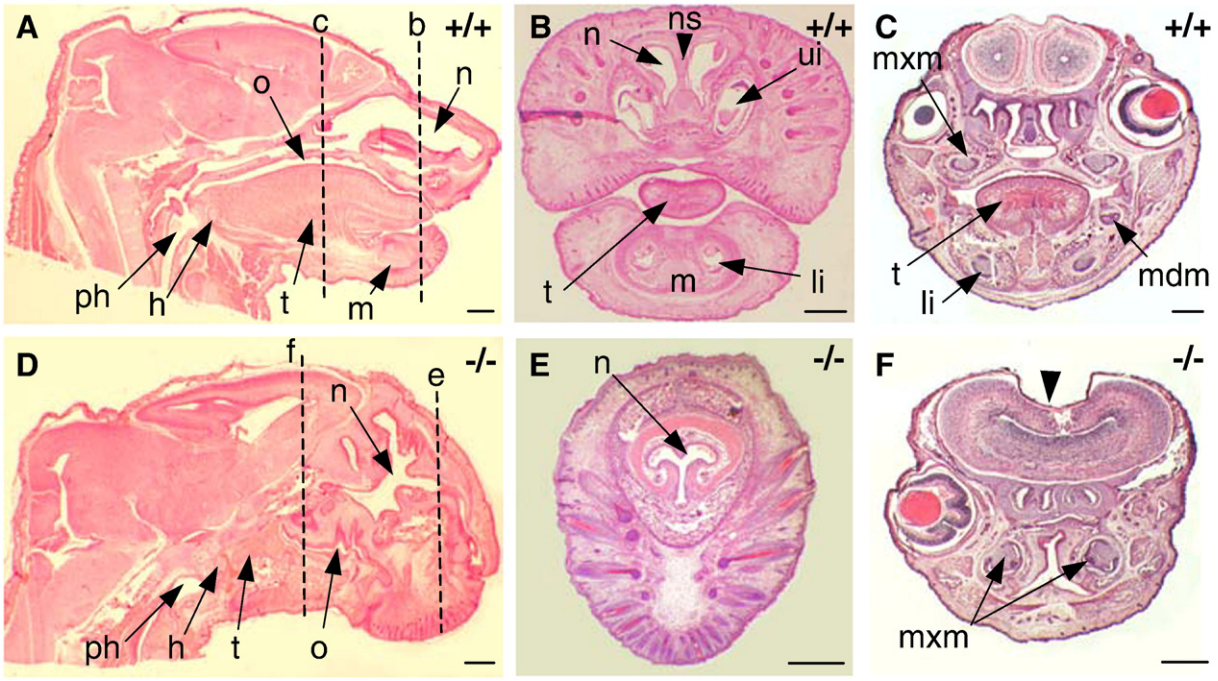

Fig. 2. Histological analysis of BA1 derivatives at birth. (A) Wild type, hematoxylin and eosin staining of a sagittal section. (B, C) Wild type, coronal sections. (D) *Twsg1*$^{-/-}$ newborn, sagittal section. Absence of the mandible (m), anterior 2/3 of the tongue (t), underdeveloped nasal (n) and oral (o) cavities, hypoplastic pharynx (ph), lack of connection between the oral cavity and the pharynx in the mutants, but preservation of the hyoid bone (h) (BA2 derivative) in the mutants. (E, F) *Twsg1*$^{-/-}$ newborn, coronal sections. Absence of the mandible (m), tongue (t), upper incisors (ui), lower incisors (li), mandibular molars (mdm), and nasal septum (ns) in the mutants. Preservation of maxillary molars (mxm) in the mutants. Dashed lines with corresponding letters indicate the level of sectioning. Scale bar: 0.5 mm.

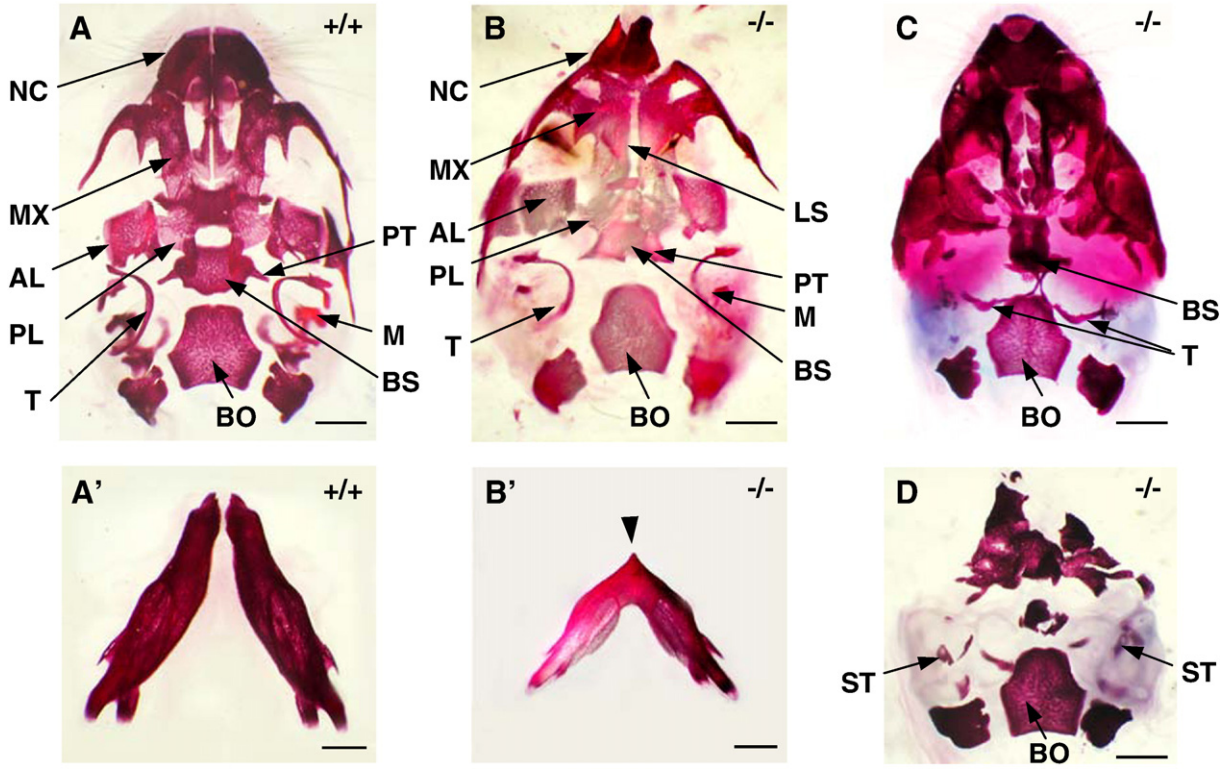

Fig. 3. Ventral views of the whole-mount skull stained with alizarin red. (A) Wild-type ventral skull with normal mandibular bones (A′) at birth. (B–D) *Twsg1*$^{-/-}$ skulls; (B) Ventral skull of *Twsg1*$^{-/-}$ newborn mouse with micrognathia showing deformity of the nasal capsule (NC), a longitudinal slit (LS) in the skull base, and preservation of the malleus (M) and pterygoid (PT). (B′) Mandible in a micrognathic *Twsg1*$^{-/-}$ newborn mouse; the mandibular bones are fused in the midline indicated by an arrow. (C) Midline fusion of the right and left tympanic bones (T) in the agnathic *Twsg1*$^{-/-}$ mouse. (D) Loss or deformity of the majority of skeletal elements anterior to basioccipital (BO) with preservation of stapes (ST) in the *Twsg1*$^{-/-}$ mouse with anterior truncation phenotype. AL, alisphenoid; BS, basisphenoid; MX, maxilla; PL, palatine. Scale bar: 1 mm.

BA2 gives rise to most of the hyoid bone, the stapes, and styloid process (Qiu et al., 1997). The BA2-derived stapes was present even in severely affected *Twsg1*$^{-/-}$ mice (Fig. 3D). The presence of the stapes and hyoid bone (Fig. 2D) suggests that BA2 development is not affected, consistent with normal histological appearance at E9.5 (Petryk et al., 2004).

Spectrum of midline fusion of BA1

To classify the phenotypic variability and determine the timing of BA1 phenotype development in *Twsg1*$^{-/-}$ mice, we examined wild type (Figs. 4A, A′) and mutant (Figs. 4B–D and B′–D′) embryos (N=40) at E9.5. BA1 is not visible in mouse embryos until around E9.0 (Thomas et al., 1998). We show that BA1 segregated into maxillary and mandibular components in *Twsg1* mutants (Figs. 4B′–D′). The majority of mutant embryos had a normal BA1 development (Figs. 4B, B′). We referred to this group of embryos as Class A. About 25% had mild (partial) fusion (Class B) of the mandibular components of BA1 (Figs. 4C, C′), and 13% had a severe midline fusion (Class C) of BA1 (Figs. 4D, D′). Similar classes were also observed at E10.5 (Class C is shown in Fig. 4F compared to Fig. 4E).

Proximo-distal marker expression in mutant mandibular arches

To examine how deficiency of TWSG1 affects proximo-distal marker expression in BA1, we compared the expression of region-specific genes in wild type and mutant embryos of Class B or C. While the expression of the distal markers *Msx1* (MacKenzie et al., 1991) and *eHand* (Cserjesi et al., 1995) was lost in the mutants (Figs. 5G, H, N, P compared to Figs. 5E, F, M, O), the expression of *Bmp4* (Winnier et al., 1995) and *Msx2* (MacKenzie et al., 1992) was preserved, albeit shifted ventrally (Figs. 5C, D, K, L compared to A, B, I, J). To examine whether gene expression is affected in the proximal region, we used the proximal markers *Fgf8* (Crossley and Martin, 1995) and *Barx1* (Tissier-Seta et al., 1995), which is downstream from *Fgf8*. The expression of these markers was preserved in the proximal regions of class B mutant BA1 (Figs. 6C, D, I, J), but unlike wild type embryos (Figs. 6A, B, G, H), the expression domain of *Fgf8* and *Barx1* extended distally across the fused BA1. In *Twsg1*$^{-/-}$ embryos with severe midline fusion (class C), *Fgf8* was reduced in the proximal region, but distal expression was preserved (Figs. 6E, F).

Given the central role that the level of BMP signaling has on the patterning of the mandibular arches, we analyzed the expression pattern of genes encoding BMP inhibitors, *Nog* and *Chrd* in wild type and *Twsg1* mutant embryos. At E9.5, the levels and distribution of *Chrd* and *Nog* transcripts were low and not appreciably different between wild type and mutant *Twsg1* embryos (not shown). The level of *Chrd* expression remained low at E10.5, with no differences between wild type and mutant embryos (not shown). The expression of *Nog* became more defined and localized to the oral epithelium at E10.5 in wild type embryos (Figs. 6K, L), as previously published (Stottmann et al., 2001) and extended across the fused BA1 in *Twsg1*$^{-/-}$ embryos (Figs. 6M, N), mimicking *Fgf8* expression.

Apoptosis is increased in the distal region of the mandibular arch in Twsg1$^{-/-}$ *embryos*

To understand the mechanism underlying the variable loss of BA1 derivatives, we examined programmed cell death within BA1. We observed only a few apoptotic cells in both the wild type (Fig. 7A) and the normal-appearing Class A mutant embryos (Fig. 7B). However, apoptosis was noticeably increased in fused mandibular arches of mutant embryos. There was a range in the extent of apoptosis with the majority of apoptotic cells accumulating in the most distal region of the mutants, with variable extension toward the proximal region in some mutants (Figs. 7C–E).

Since signaling within BA1 is regionalized, and because BMPs are critical for the development of the distal region, we designed a method to quantify apoptosis that would reflect this regionalization. We defined the distal region as the middle third of BA1 (Figs. 7F, G). When we quantified apoptosis by distal and proximal regions, we found a 10-fold increase in the apoptotic index in the distal region of the mandibular arch in *Twsg1*$^{-/-}$ embryos compared to wild type embryos (19.7±13.6 vs. 1.9±1.4, p<0.01) (Fig. 7H). The difference between the apoptotic index in the distal versus proximal regions of the mutants was also statistically significant (19.7±13.6 vs. 6.2±2.3, p<0.01; data not shown). There was no significant difference between the apoptotic index in the distal versus proximal regions in wild type embryos. Although there was a trend towards increased apoptosis in the proximal region of the mutants compared to wild type embryos (2.5-fold), it was not statistically significant. These results suggested that the increase in apoptosis was regionalized in *Twsg1*$^{-/-}$ embryos with the most significant increase in apoptosis in the distal region. We did not detect significant differences in proliferation between wild type and mutant BA1 (data not shown).

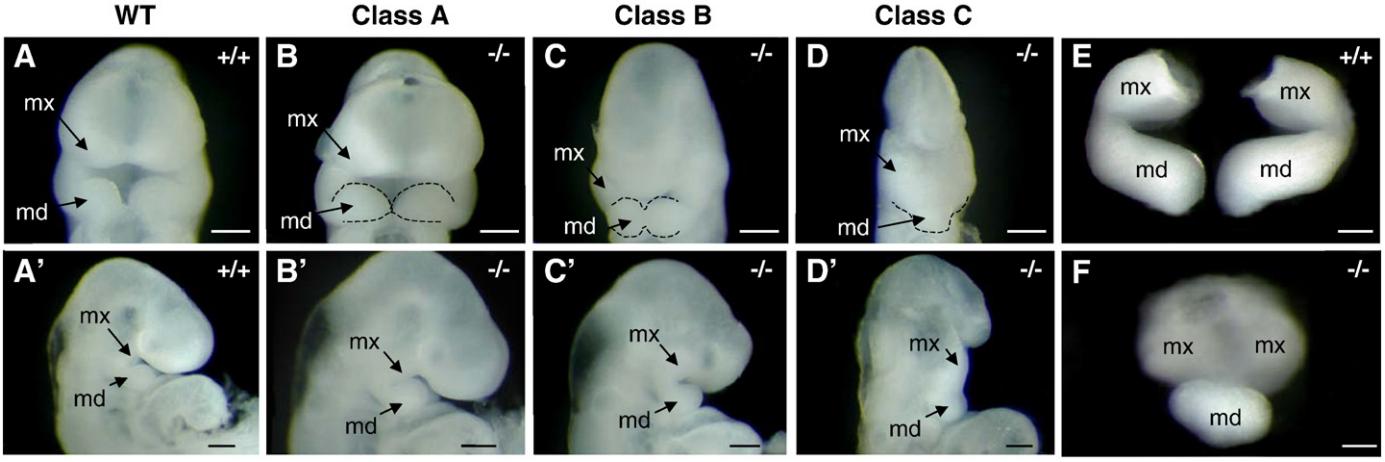

Fig. 4. Spectrum of BA1 fusion in *Twsg1*$^{-/-}$ embryos at E9.5. (A, A′) Wild type embryo in frontal and lateral views. (B, B′–D, D′) Three classes of *Twsg1* mutants. Class A — normal appearance of the BA1; Class B — partial midline fusion of BA1 with some preservation of the forebrain; Class C — severe midline fusion with ventral displacement of BA1 and severe reduction of anterior head structures. (E) Micro-dissected wild type BA1 at E10.5. (F) Mutant BA1 class C with severe midline fusion of the mandibular components and only partial separation of the maxillary components at E10.5. Dashed lines outline the mandibular prominences of BA1; mx, maxillary component of BA1; md, mandibular component of BA1. Scale bar: 200 μm.

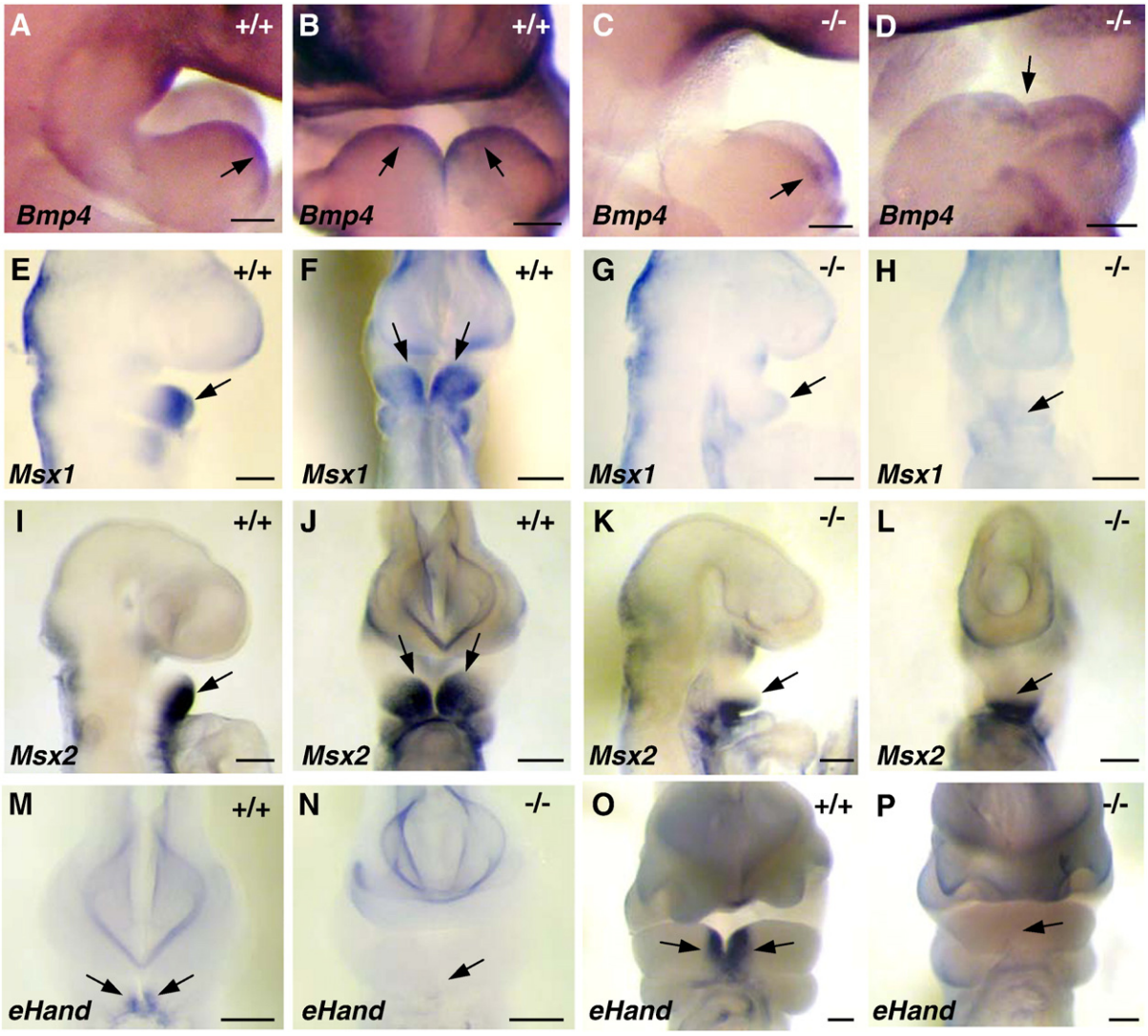

Fig. 5. Expression of distal markers in wild type and medially fused mutant BA1. (A, B) Lateral and frontal views of wild type *Bmp4* expression in the distal region at E9.5. (C, D) Distal expression of *Bmp4* is preserved in *Twsg1* mutants but is shifted ventrally. (E, F) Lateral and frontal views of wild type *Msx1* expression in the distal region at E9.5. (G, H) Distal expression of *Msx1* is lost in the mutants at E9.5. (I, J) Gradient of wild type *Msx2* expression in the distal region at E9.5; lateral and frontal views. (K, L) Distal expression of *Msx2* is preserved in *Twsg1* mutants and it is shifted ventrally. Note diffuse expression of *Msx2* across BA1. (M) Wild type *eHand* expression in the distal region at E9.5. (N) Loss of distal expression of *eHand* in *Twsg1*$^{-/-}$ embryo at E9.5. (O) Wild type *eHand* expression in the distal region at E10.5. (P) Loss of distal expression of *eHand* in *Twsg1*$^{-/-}$ embryo at E10.5. Scale bar: 100 μm in A–D and 200 μm in E–P.

TWSG1 deficiency results in a loss of the BMP signaling gradient within BA1

SMAD1/5/8 phosphorylation by type I BMP receptor is a key step in BMP signal transduction and is indicative of the level of BMP signaling (Chen et al., 2004). To examine the level and distribution of BMP signaling during initial and critical periods of BA1 morphogenesis at E9.5, we performed immunostaining to detect pSMAD1/5. In wild type embryos, pSMAD1/5 immunostaining was distributed in a proximo-distal gradient, which was highest in the distal region and decreased toward the proximal region (Figs. 8A–C), similar to previous reports (Liu et al., 2005). The pattern of signal distribution was mosaic and similar to the published result using pSMAD1/5/8 antibody (Di-Gregorio et al., 2007) when tested at E7.5 (not shown). In *Twsg1*$^{-/-}$ embryos, the distribution of pSMAD1/5 immunostaining was distinct from the pattern shown in wild type embryos. The characteristic gradient of BMP signaling was disrupted in the mutants, resulting in more diffuse signaling, which was also shifted ventrally (Figs. 8D, E). Interestingly, *Msx2*, a downstream target of BMP signaling, was also shifted ventrally, forming an expression domain across the distal BA1 (Figs. 5K, L).

Discussion

The effect of TWSG1 deficiency on proximo-distal marker expression in BA1

Gene expression within BA1 is organized in a proximo-distal fashion (Fig. 9A) and is regulated by two main signaling pathways: BMP and FGF8; although other pathways are also involved (Ferguson et al., 2000; Jiang et al., 2006; Mina et al., 2002). At E9.5, *Bmp4* is expressed in the epithelium of the distal region and *Fgf8* is expressed in the epithelium of the proximal region (Tucker and Sharpe, 2004). While the expression of *Fgf8* remains in the proximal domain, *Bmp4* expression shifts from the oral epithelium to the mesenchyme and extends into a more proximal domain of the presumptive molar region between E10.5 and E11.5 (Tucker et al., 1998a). In the developing BA1, epithelial gene expression regulates transcription of

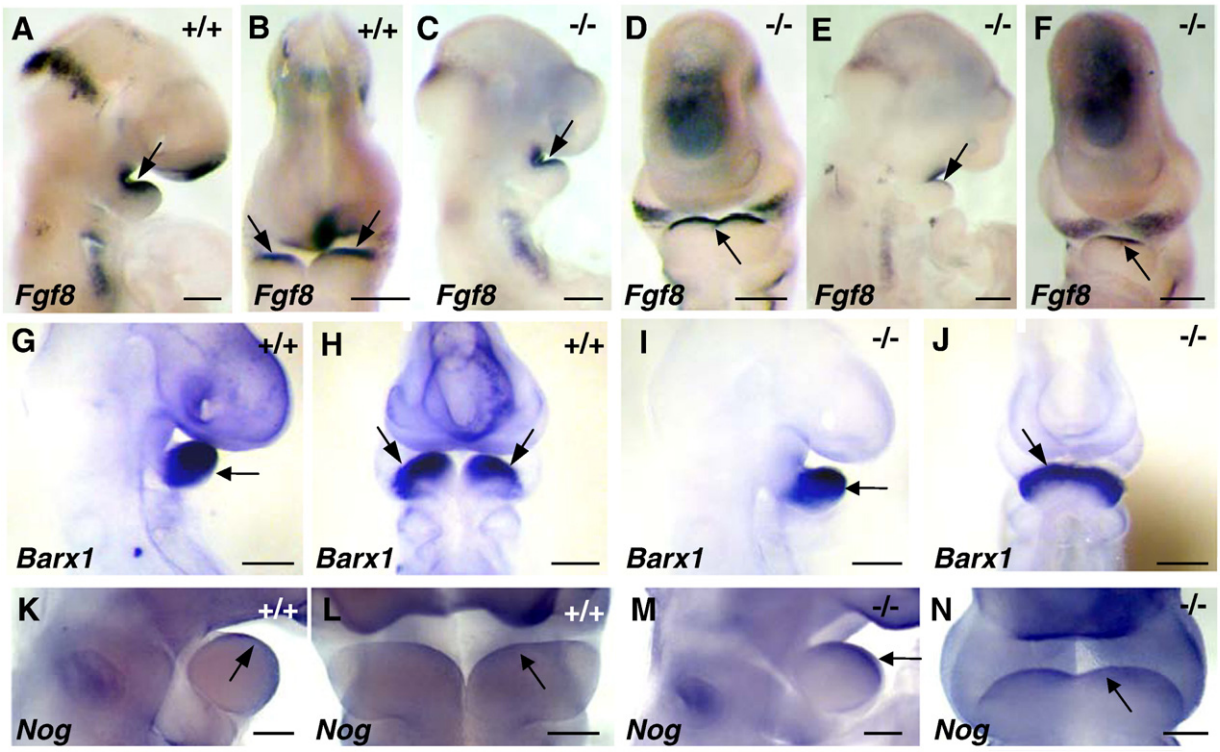

Fig. 6. Expression of proximal markers in wild type and fused mutant BA1. (A, B) Lateral and frontal views of wild type *Fgf8* expression in the oral epithelium of the proximal region of BA1 at E9.5. (C, D) The expression of *Fgf8* is preserved in the proximal region of mutant embryos of class B and extends across the fused BA1 tissue, reflecting a shift of expression domain. (E, F) The expression of *Fgf8* is significantly reduced in the proximal region of mutant embryos of class C, but present in the distal region. (G, H) Lateral and frontal views of wild type *Barx1* expression in the mesenchyme of the proximal region of BA1 at E9.5. (I, J) Expression domain of *Barx1* is extended across the midline in *Twsg1* mutants. (K, L) Lateral and frontal views of wild type *Nog* expression in the oral epithelium of BA1 at E10.5. (I, J) Expression of *Nog* is extended across the fused BA1 in *Twsg1*$^{-/-}$ embryos. Scale bar: 200 μm in A–J and 100 μm in K–N.

downstream mesenchymal genes. *Msx1* and *Msx2* are direct transcription targets of BMP signaling in the distal mesenchyme (Tucker et al., 1998a; Vainio et al., 1993). Likewise, *Barx1* expression is induced by FGF8 in the proximal region (Tucker et al., 1998b). *Msx1* also receives transcriptional input from another signaling cascade involving ET-1 and dHAND/eHAND (Thomas et al., 1998).

BMP4 regulates *Fgf8* expression in a dose-dependent manner: a high level of BMP4 represses *Fgf8* expression in the distal region, while a low level of BMP4 signaling maintains *Fgf8* expression in the proximal region (Liu et al., 2005). Inactivation of *Bmp4* in the mandibular ectoderm and pharyngeal endoderm (*Nkx2.5cre;Bmp4*$^{n/f}$) results in severely reduced BMP signaling. In these mutants, there is not enough BMP4 present to either maintain *Fgf8* expression in the proximal region or to repress it in the distal region (Liu et al., 2005). Thus, the expression of *Fgf8* (as well as its target *Barx1*) is lost in the proximal region in mutant BA1 at E10.5, but maintained in the distal region due to lack of repression by BMP4. Unlike *Bmp4* mutant embryos, *Twsg1* homozygous mutants show *Fgf8* (and *Barx1*) expression that is present in the proximal region and expanded into the distal region (Fig. 9B). This suggests that the level of BMP signaling is sufficient to maintain *Fgf8* expression in the proximal region of BA1 in the mutants. Lack of repression of *Fgf8* transcription in the distal region of fused BA1 is likely due to ventral shift of both *Bmp4* expression domain and BMP signaling.

The BMP4 target genes, *Msx1* and *Msx2*, have different BMP4 dosage requirements, such that *Msx2* transcription requires higher levels of BMP signaling than *Msx1*. In *Bmp4* mutants, the expression of *Msx2* is lost, while expression of *Msx1* is maintained (Liu et al., 2005), suggesting residual low level of BMP signaling, which is sufficient for *Msx1* expression. That *Msx1* expression is maintained in *Bmp4* mutants could be due to other BMP signals such as BMP7. However, in *Wnt1-Cre;Smad4*$^{fl/fl}$ mutants, in which *Smad4* is deleted in the neural crest derived mesenchymal cells, both *Msx1* and *Msx2* expression are lost, which is consistent with further reduction in BMP signaling (Ko et al., 2007). Thus, the presence of *Msx2* expression in *Twsg1*$^{-/-}$ BA1 indicates that the level of BMP signaling is above the threshold required for *Msx2* transcription. Loss of *Msx1* may be explained by the loss of the most distal BA1 marker *eHand*, which is also upstream from *Msx1*.

In summary, changes in gene expression are most pronounced in the distal region of the mandibular arch in *Twsg1*$^{-/-}$ embryos and correspond to a shift in the distribution of *Bmp4* transcript and signaling. These observations are consistent with a role of BMPs in defining the morphogenetic field within distal BA1.

Alteration of BMP morphogenetic field in the mandibular arch of Twsg1$^{-/-}$ *embryos*

The BMP signaling gradient plays a critical role in embryonic development of invertebrate and vertebrate species by determining direction of cell migration, transcription of genes, cell competition, cell survival and proliferation (Bollenbach et al., 2008; Moreno et al., 2002; Muller et al., 2003; O'Connor et al., 2006; Tucker et al., 2008; von der Hardt et al., 2007). Mandibular development in mouse and chick embryos has been shown to be sensitive to a BMP signaling threshold as well as the timing and location of BMP signaling (Ekanayake and Hall, 1997; Liu et al., 2005; Mina et al., 2002). For example, BMP4 has a dual function in the regulation of *Fgf8* expression. Higher levels of BMP4 repress *Fgf8* expression in the distal region, while lower levels maintain *Fgf8* expression in the proximal region (Liu et al., 2005), corresponding to the distribution of BMP signaling gradient within the mesenchyme of BA1.

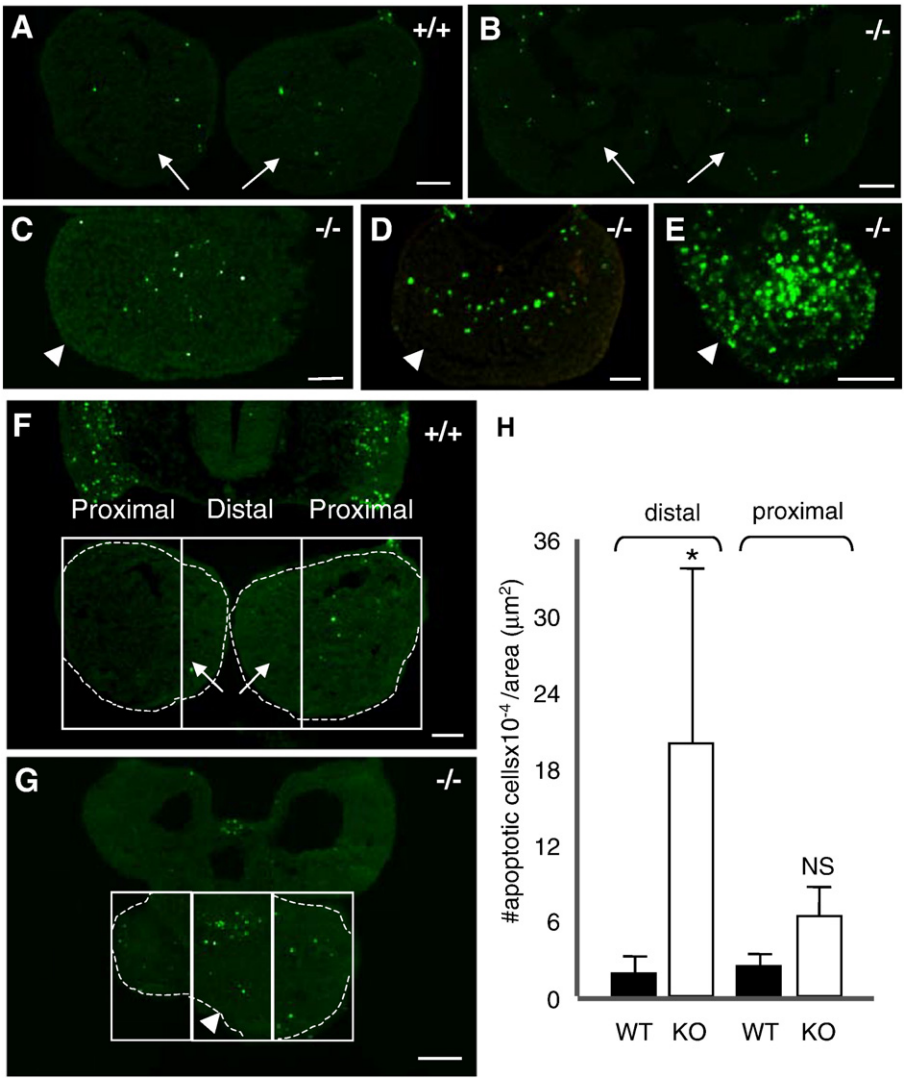

Fig. 7. Range of apoptosis in BA1 at E9.5. (A) Minimal apoptosis in wild type BA1. (B–E) Apoptosis in *Twsg1*$^{-/-}$ mutants. (B) Apoptosis in normal-appearing mutant BA1 is comparable to apoptosis in wild type BA1. (C) Increased apoptosis in the most distal part of mutant BA1. (D) More extensive apoptosis into the proximal region of mutant BA1. (E) Largely increased apoptosis throughout BA1 in the mutant. (F–H) Quantification of apoptosis. Comparison of apoptosis between wild type (F) and *Twsg1* mutant (G) embryos at E9.5. The distal region was defined as the middle third of BA1. The area of each section was outlined within each box (dashed lines) and apoptotic cells were counted at 200× in each section per area (apoptotic index). (H) Data are expressed as the mean ± s.d. There was a significant 10-fold increase (*$p < 0.01$) in apoptotic index in the distal region of the mutant vs. wild type BA1. Arrows point to mandibular prominences of BA1 and arrowheads point to the fused BA1. NS, not statistically significant, scale bar: 50 μm.

It is not clear how the gradient of BMP signaling is established within the BA1, but there is evidence that BMP-binding proteins, such as TWSG1, CHRD, NOG, Crossveinless-2, Chordin-like-1, and Chordin-like-2 play a role in shaping BMP gradient in other regions during mouse embryonic development (e.g. vertebrae) (Zakin et al., 2008) and other model organisms (Ben-Zvi et al., 2008; Little and Mullins, 2006; Nakayama et al., 2004; O'Connor et al., 2006; Serpe et al., 2008; Zhang et al., 2008). For example, Tsg and Sog (homologue of CHRD) contribute to the formation of a Dpp (homologue of vertebrate BMP) gradient in *Drosophila* (Ross et al., 2001). While BMP-binding proteins are typically thought of as BMP inhibitors since they sequester BMPs from their receptors, it has recently been suggested that they may also provide a mode of delivery of BMPs to areas that require peak BMP levels (O'Connor et al., 2006). Shaping of the Dpp gradient involves not only interactions with binding proteins and proteases, but also relies on the source of synthesis, concentration gradients of extracellular proteins and their diffusion away from the site of synthesis (O'Connor et al., 2006; Srinivasan et al., 2002).

We have observed a disruption of the BMP4 gradient in the absence of TWSG1, which suggests a role for TWSG1 in establishing this gradient. Between E9.5 and E10.5, *Twsg1* is expressed diffusely throughout BA1 mesenchyme, with slight gradient formation toward the distal region at E10.5 (at both mRNA and protein level). By E11.5, *Twsg1* shifts toward the oral epithelium and into the proximal region. Simultaneously, *Bmp4* expression shifts from the oral epithelium to the mesenchyme and extends proximally into the presumptive molar region (Tucker et al., 1998a). BMP4 presumably diffuses from the site of synthesis and activates SMAD1,5,8 in the mesenchyme of the distal region. Inhibition of BMP signaling by TWSG1 (and perhaps other BMP-interacting proteins) would be more likely to occur away from the site of synthesis where the BMP4 level would be expected to be low (indicated by a dashed oval in Fig. 9A) and thereby prevent further diffusion of the BMP gradient. This argument would provide a mechanism to support the anti-BMP activity of TWSG1. However, we cannot exclude the possibility that TWSG1 could also bind BMP4 in the most distal region and help concentrate the ligand to promote peak BMP activity in that region (indicated by a dotted oval in Fig. 9A), alone or in combination with other proteins. This mechanism is similar to the one recently proposed for another BMP-interacting protein Crossveinless-2 in

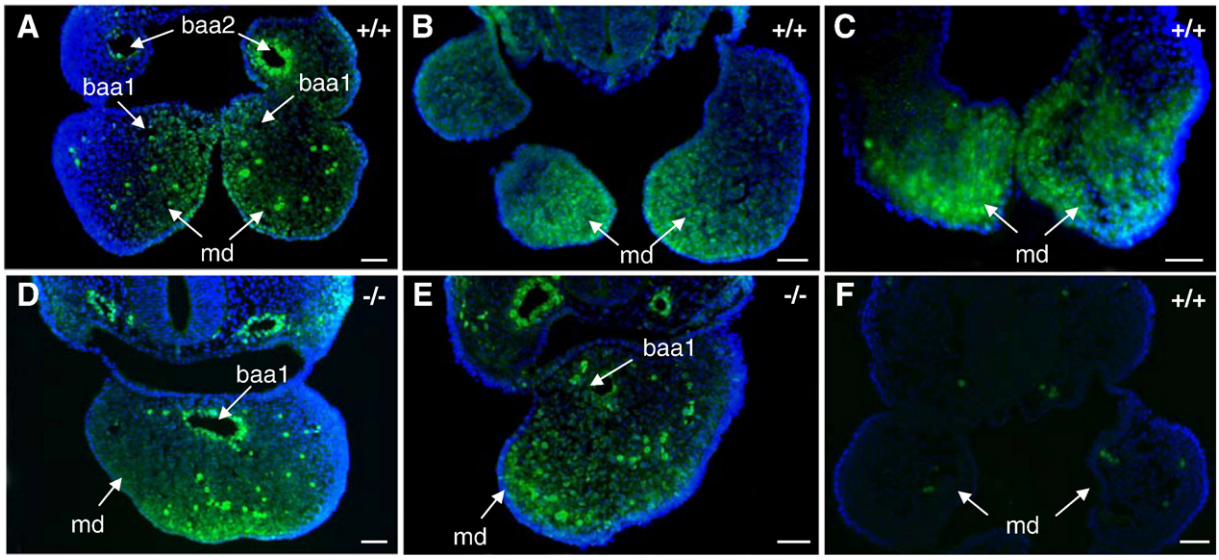

Fig. 8. Distribution of pSMAD1/5 in BA1 at E9.5. (A–C) In wild type embryos, pSMAD1/5 immunostaining is distributed in a gradient, which is highest in the distal region and decreases proximally. (D, E) BMP signaling gradient is disrupted and shifted ventrally in *Twsg1*$^{-/-}$ embryos. (F) Negative control (no anti-pSMAD1/5 antibody). Few individual non-specifically staining cells can be seen. Scale bar: 50 μm.

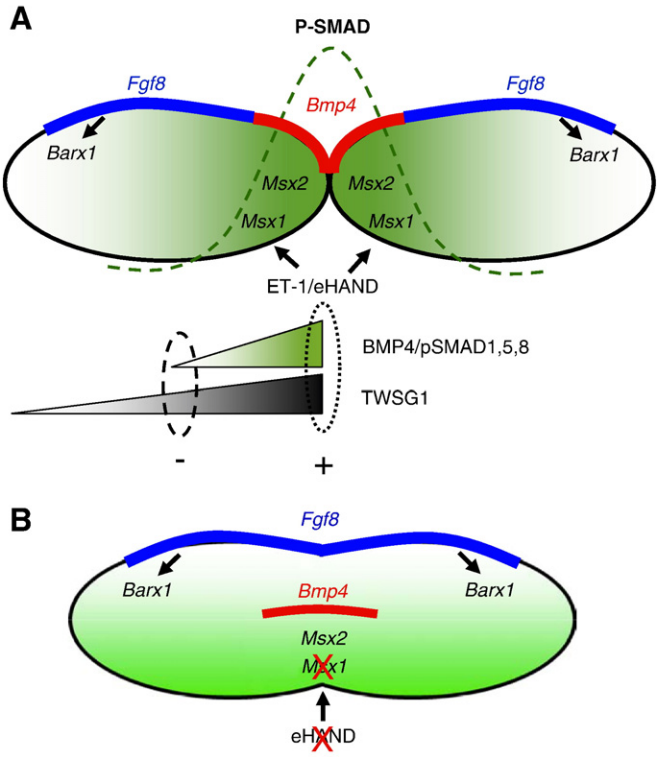

Fig. 9. Model of proximo-distal gene expression and BMP signaling in wild type and *Twsg1* mutant BA1 at E9.5–E10.5. (A) Wild type. *Bmp4* is expressed in the oral epithelium in the distal region and *Fgf8* is expressed in the epithelium in the proximal region. *Msx1* and *Msx2* are downstream targets of BMP signaling in the distal region. *Msx1* also receives input from ET-1/eHAND. Gradient of BMP activity is indicated by green shading and a dashed line. Inhibition of BMP signaling by BMP-interacting proteins, for example TWSG1, would be more likely away from the site of synthesis where BMP4 level would be expected to be low (indicated by a dashed oval) to prevent further diffusion of BMP gradient. Alternatively, the role of BMP-binding proteins would be to help concentrate the ligand in the distal region to promote peak BMP activity in that region (indicated by a dotted oval). (B) Abnormally fused BA1 in *Twsg1*$^{-/-}$ embryo. *Bmp4* as well as *Msx2* expression is shifted ventrally. Loss of *Msx1* expression may be secondary to loss of *eHand* expression. *Fgf8* expression extends across the fused BA1. Ventral shift in *Bmp4* expression is accompanied by disruption of BMP gradient and altered distribution of BMP signaling.

the formation of a BMP morphogenetic gradient in the vertebral body cartilage (Zakin et al., 2008).

While the distribution of BMP signaling is shifted in *Twsg1* mutants (Fig. 9B), it should be pointed out that the overall level of BMP signaling in BA1 of the mutants cannot be determined from pSMAD1/5 immunostaining. An alternative explanation is that there is a disruption of the BMP gradient at the level of signaling as well as mRNA expression due to a mis-specification of certain cell types in the mutant BA1. Therefore the change in the distribution of pSMAD1/5 that we observed could be either a direct result of the loss of TWSG1 or secondary to the patterning defects present in the *Twsg1* mutants. Altered distribution of BMP signaling in *Twsg1*$^{-/-}$ embryos leads to a shift in gene expression (e.g. *Msx2*) resulting in a significant increase in apoptosis in the distal region.

Apoptosis as a mechanism of phenotypic variability and limited distal outgrowth

An interesting and perplexing feature of many human craniofacial syndromes is phenotypic variability as a result of a single gene mutation, which can occur even within the same family. For example, patients with Treacher–Collins syndrome or holoprosencephaly have an extremely wide range of clinical presentation from very mild clinical signs to severe craniofacial abnormalities (Hansen et al., 1996; Hehr et al., 2004; Roessler et al., 1996). Mice deficient in TWSG1 also have a spectrum of craniofacial defects ranging from micrognathia to agnathia, accompanied by positioning of the ears toward the midline, midline facial defects, and holoprosencephaly (Petryk et al., 2004; Schiffer et al., 2002); a constellation of findings that resembles human agnathia–otocephaly complex. While the basis of this variability is likely to be complex and involve both genetic interactions and epigenetic phenomena, we investigated apoptosis as one of possible mechanisms.

We hypothesized that impaired development of the mandible in *Twsg1*$^{-/-}$ mice could result from BMP-induced apoptosis. It is known that ectopic application of BMP2 or BMP7 to chick mandibular processes early in development induces apoptosis, ectopic expression of *Msx* genes, and inhibition of mandibular outgrowth (Ekanayake and Hall, 1997; Mina et al., 2002). *Msx2* is thought to mediate pro-apoptotic effects of BMPs (Marazzi et al., 1997; Mina et al., 1995). We found that in *Twsg1* mutants, *Bmp4* and *Msx2* expression persisted in

the distal region in addition to being shifted ventrally. Diffuse level of BMP signaling in *Twsg1*$^{-/-}$ embryos activates *Msx2*, thereby inducing apoptosis. Proximo-distal extension of apoptosis may be one of the mechanisms to account for variable loss of BA1 derivatives.

Limited distal outgrowth due to apoptotic elimination of predominantly distal tissue likely leads to the appearance of premature/accelerated fusion of BA1. While inadequate outgrowth of the palatal shelves would prevent midline contact and fusion, leading to cleft palate (Satokata and Maas, 1994; Welsh et al., 2007), inadequate outgrowth of BA1 is more likely to result in premature midline contact and fusion of mandibular prominences, leading to micrognathia or agnathia. In fact, any combination of factors taking place within BA1, including excessive apoptosis or inadequate proliferation, or even before the neural crest cells populate the branchial arches would be expected to have the same end-point, which is BA1 hypoplasia and micrognathia. These differences in preferred developmental responses to inadequate outgrowth of palatal shelves versus distal BA1 could explain the common occurrence of cleft palate (1 in 1000 infants) (Lan et al., 2007) and micrognathia as opposed to the rarity of mandibular clefts in mice and humans (Oostrom et al., 1996).

At present, the molecular mechanisms that control midline BA1 fusion are unknown. It has been speculated that local growth factors may signal to the midline epithelial cells in either a paracrine or autocrine fashion both to evoke their migration and to facilitate interruption of the extracellular matrix which is evident at the initiation of fusion (Chai et al., 2000). The expression of *Bmp4* in the midline epithelium, the ability of the BMP signaling gradient to determine direction of cell migration (von der Hardt et al., 2007), and the variable defects in mandibular fusion in mice with mutations affecting the BMP pathway all provide evidence to support this pathway as a likely regulator of midline fusion. For example, *Nkx2.5cre; Bmp4*$^{n/f}$ mutants have midline fusion of mandibular bones (Liu et al., 2005), similar to *Twsg1*$^{-/-}$ mice. Some *Chrd*$^{-/-}$;*Nog*$^{-/-}$ mutants also have fused BA1 (Stottmann et al., 2001). Only a severe reduction in BMP signaling level, for example in *Wnt1-Cre;Smad4*$^{f/f}$ mutants (Ko et al., 2007) or *Msx1*$^{-/-}$;*Msx2*$^{-/-}$ compound mutants (Ishii et al., 2005), results in failure of midline fusion of BA1 and mandibular clefts in the latter mutant.

In summary, our results demonstrate the importance of TWSG1 in the development of BA1 and shed light on the mechanisms underlying abnormal BA1 development that may lead to micrognathia or agnathia. Although the work described focuses on the molecular and cellular processes within the mandibular arch of *Twsg1* mutants, morphogenesis of BA1 is a multi-step process that begins before the actual appearance of BA1 at E9.0. The process begins with the formation and delamination of cephalic neural crest cells and their subsequent migration to BA1 in close proximity to the pharyngeal endoderm. Both of these steps could be perturbed, in addition to abnormal signaling within the BA1 of *Twsg1*$^{-/-}$ mice. The similarity of ventral skull and mandibular defects between *Twsg1*$^{-/-}$ mice and *Otx2*$^{+/-}$ mice (Kuratani et al., 1997; Matsuo et al., 1995) suggests that there may be an additional midbrain neural crest defect that limits the number of neural crest cells populating the distal region, and thus limiting distal outgrowth, which will be addressed in future studies.

Acknowledgments

The authors thank Dr. Michael O'Connor for critical review of the manuscript, Dr. Walter Sebald for helpful discussions, Dr. Wei Liu for the *Barx1* probe, Dr. Eric Olson for the *eHand* probe, Dr. John Klingensmith for the *Bmp4* and *Nog* probes, and Dr. Mark Ferguson for the *Msx2* probe. The assistance with lab procedures of Janine Gessner and Michael Jarcho is most appreciated. This project was supported by a 3M Science and Technology Fellowship and Block grant from the University of Minnesota Graduate School to B.M., R01DE016601 to A.P., and the Academic Health Center seed grant to R.G., R.W. was supported by the Minnesota Craniofacial Research Training Program (MinnCResT) T32DE007288 and C.J.B. was supported by the Musculoskeletal Training Grant NIH-NIAMS, T32 AR050938.

References

Ben-Zvi, D., Shilo, B.Z., Fainsod, A., Barkai, N., 2008. Scaling of the BMP activation gradient in *Xenopus* embryos. Nature 453, 1205–1211.
Bollenbach, T., Pantazis, P., Kicheva, A., Bokel, C., Gonzalez-Gaitan, M., Julicher, F., 2008. Precision of the Dpp gradient. Development 135, 1137–1146.
Cerny, R., Lwigale, P., Ericsson, R., Meulemans, D., Epperlein, H.H., Bronner-Fraser, M., 2004. Developmental origins and evolution of jaws: new interpretation of "maxillary" and "mandibular". Dev. Biol. 276, 225–236.
Chai, Y., Sasano, Y., Bringas Jr., P., Mayo, M., Kaartinen, V., Heisterkamp, N., Groffen, J., Slavkin, H., Shuler, C., 1997. Characterization of the fate of midline epithelial cells during the fusion of mandibular prominences in vivo. Dev. Dyn. 208, 526–535.
Chai, Y., Jiang, X., Ito, Y., Bringas Jr., P., Han, J., Rowitch, D.H., Soriano, P., McMahon, A.P., Sucov, H.M., 2000. Fate of the mammalian cranial neural crest during tooth and mandibular morphogenesis. Development 127, 1671–1679.
Chen, D., Zhao, M., Mundy, G.R., 2004. Bone morphogenetic proteins. Growth Factors 22, 233–241.
Chung, C.S., Myrianthopoulos, N.C., 1975. Factors affecting risks of congenital malformations. I. Analysis of epidemiologic factors in congenital malformations. Report from the Collaborative Perinatal Project. Birth Defects Orig. Artic Ser. 11, 1–22.
Crossley, P.H., Martin, G.R., 1995. The mouse Fgf8 gene encodes a family of polypeptides and is expressed in regions that direct outgrowth and patterning in the developing embryo. Development 121, 439–451.
Cserjesi, P., Brown, D., Lyons, G.E., Olson, E.N., 1995. Expression of the novel basic helix–loop–helix gene eHAND in neural crest derivatives and extraembryonic membranes during mouse development. Dev. Biol. 170, 664–678.
Depew, M.J., Lufkin, T., Rubenstein, J.L., 2002. Specification of jaw subdivisions by Dlx genes. Science 298, 381–385.
Di-Gregorio, A., Sancho, M., Stuckey, D.W., Crompton, L.A., Godwin, J., Mishina, Y., Rodriguez, T.A., 2007. BMP signalling inhibits premature neural differentiation in the mouse embryo. Development 134, 3359–3369.
Dixon, J., Trainor, P., Dixon, M.J., 2007. Treacher Collins syndrome. Orthod. Craniofac. Res. 10, 88–95.
Ekanayake, S., Hall, B.K., 1997. The in vivo and in vitro effects of bone morphogenetic protein-2 on the development of the chick mandible. Int. J. Dev. Biol. 41, 67–81.
Ferguson, C.A., Tucker, A.S., Sharpe, P.T., 2000. Temporospatial cell interactions regulating mandibular and maxillary arch patterning. Development 127, 403–412.
Gazzerro, E., Deregowski, V., Stadmeyer, L., Gale, N.W., Economides, A.N., Canalis, E., 2006. Twisted gastrulation, a bone morphogenetic protein agonist/antagonist, is not required for post-natal skeletal function. Bone 39, 1252–1260.
Hansen, M., Lucarelli, M.J., Whiteman, D.A., Mulliken, J.B., 1996. Treacher Collins syndrome: phenotypic variability in a family including an infant with arhinia and uveal colobomas. Am. J. Med. Genet. 61, 71–74.
Hehr, U., Gross, C., Diebold, U., Wahl, D., Beudt, U., Heidemann, P., Hehr, A., Mueller, D., 2004. Wide phenotypic variability in families with holoprosencephaly and a sonic hedgehog mutation. Eur. J. Pediatr. 163, 347–352.
Hogan, B., Beddington, R., Constantini, F., Lacy, E., 1994. Manipulating the mouse embryo. A laboratory manual. Cold Spring Harbor Laboratory Press, New York.
Ishii, M., Han, J., Yen, H.Y., Sucov, H.M., Chai, Y., Maxson Jr., R.E., 2005. Combined deficiencies of Msx1 and Msx2 cause impaired patterning and survival of the cranial neural crest. Development 132, 4937–4950.
Jiang, R., Bush, J.O., Lidral, A.C., 2006. Development of the upper lip: morphogenetic and molecular mechanisms. Dev. Dyn. 235, 1152–1166.
Ko, S.O., Chung, I.H., Xu, X., Oka, S., Zhao, H., Cho, E.S., Deng, C., Chai, Y., 2007. Smad4 is required to regulate the fate of cranial neural crest cells. Dev. Biol. 312, 435–447.
Kuratani, S., Matsuo, I., Aizawa, S., 1997. Developmental patterning and evolution of the mammalian viscerocranium: genetic insights into comparative morphology. Dev. Dyn. 209, 139–155.
Lan, Y., Wang, Q., Ovitt, C.E., Jiang, R., 2007. A unique mouse strain expressing Cre recombinase for tissue-specific analysis of gene function in palate and kidney development. Genesis 45, 618–624.
Larrain, J., Oelgeschlager, M., Ketpura, N.I., Reversade, B., Zakin, L., De Robertis, E.M., 2001. Proteolytic cleavage of Chordin as a switch for the dual activities of Twisted gastrulation in BMP signaling. Development 128, 4439–4447.
Lee, S.H., Bedard, O., Buchtova, M., Fu, K., Richman, J.M., 2004. A new origin for the maxillary jaw. Dev. Biol. 276, 207–224.
Little, S.C., Mullins, M.C., 2006. Extracellular modulation of BMP activity in patterning the dorsoventral axis. Birth Defects Res. C Embryo Today 78, 224–242.
Liu, W., Selever, J., Murali, D., Sun, X., Brugger, S.M., Ma, L., Schwartz, R.J., Maxson, R., Furuta, Y., Martin, J.F., 2005. Threshold-specific requirements for Bmp4 in mandibular development. Dev. Biol. 283, 282–293.
MacKenzie, A., Ferguson, M.W., Sharpe, P.T., 1991. Hox-7 expression during murine craniofacial development. Development 113, 601–611.
MacKenzie, A., Ferguson, M.W., Sharpe, P.T., 1992. Expression patterns of the homeobox gene, Hox-8, in the mouse embryo suggest a role in specifying tooth initiation and shape. Development 115, 403–420.
Marazzi, G., Wang, Y., Sassoon, D., 1997. Msx2 is a transcriptional regulator in the BMP4-mediated programmed cell death pathway. Dev. Biol. 186, 127–138.

Matsuo, I., Kuratani, S., Kimura, C., Takeda, N., Aizawa, S., 1995. Mouse Otx2 functions in the formation and patterning of rostral head. Genes Dev. 9, 2646–2658.
McGonnell, I.M., Clarke, J.D., Tickle, C., 1998. Fate map of the developing chick face: analysis of expansion of facial primordia and establishment of the primary palate. Dev. Dyn. 212, 102–118.
McMahon, J.A., Takada, S., Zimmerman, L.B., Fan, C.M., Harland, R.M., McMahon, A.P., 1998. Noggin-mediated antagonism of BMP signaling is required for growth and patterning of the neural tube and somite. Genes Dev. 12, 1438–1452.
Melnick, M., Petryk, A., Abichaker, G., Witcher, D., Person, A.D., Jaskoll, T., 2006. Embryonic salivary gland dysmorphogenesis in Twisted gastrulation deficient mice. Arch. Oral Biol. 51, 433–438.
Mina, M., Gluhak, J., Upholt, W.B., Kollar, E.J., Rogers, B., 1995. Experimental analysis of Msx-1 and Msx-2 gene expression during chick mandibular morphogenesis. Dev. Dyn. 202, 195–214.
Mina, M., Wang, Y.H., Ivanisevic, A.M., Upholt, W.B., Rodgers, B., 2002. Region-and stage-specific effects of FGFs and BMPs in chick mandibular morphogenesis. Dev. Dyn. 223, 333–352.
Moreno, E., Basler, K., Morata, G., 2002. Cells compete for decapentaplegic survival factor to prevent apoptosis in *Drosophila* wing development. Nature 416, 755–759.
Moss, J.P., James, D.R., 1984. An investigation of a group of 35 consecutive patients with a first arch syndrome. Br. J. Oral Maxillofac. Surg. 22, 157–169.
Muller, B., Hartmann, B., Pyrowolakis, G., Affolter, M., Basler, K., 2003. Conversion of an extracellular Dpp/BMP morphogen gradient into an inverse transcriptional gradient. Cell 113, 221–233.
Nakayama, N., Han, C.Y., Cam, L., Lee, J.I., Pretorius, J., Fisher, S., Rosenfeld, R., Scully, S., Nishinakamura, R., Duryea, D., Van, G., Bolon, B., Yokota, T., Zhang, K., 2004. A novel chordin-like BMP inhibitor, CHL2, expressed preferentially in chondrocytes of developing cartilage and osteoarthritic joint cartilage. Development 131, 229–240.
Nanci, A., 2003. Ten Cate's Oral Histology: Development, Structure and Function. Mosby, St. Louis.
Nosaka, T., Morita, S., Kitamura, H., Nakajima, H., Shibata, F., Morikawa, Y., Kataoka, Y., Ebihara, Y., Kawashima, T., Itoh, T., Ozaki, K., Senba, E., Tsuji, K., Makishima, F., Yoshida, N., Kitamura, T., 2003. Mammalian twisted gastrulation is essential for skeleto-lymphogenesis. Mol. Cell. Biol. 23, 2969–2980.
O'Connor, M.B., Umulis, D., Othmer, H.G., Blair, S.S., 2006. Shaping BMP morphogen gradients in the *Drosophila* embryo and pupal wing. Development 133, 183–193.
Oelgeschlager, M., Reversade, B., Larrain, J., Little, S., Mullins, M.C., De Robertis, E.M., 2003. The pro-BMP activity of Twisted gastrulation is independent of BMP binding. Development 130, 4047–4056.
Oostrom, C.A., Vermeij-Keers, C., Gilbert, P.M., van der Meulen, J.C., 1996. Median cleft of the lower lip and mandible: case reports, a new embryologic hypothesis, and subdivision. Plast. Reconstr. Surg. 97, 313–320.
Petryk, A., Anderson, R.M., Jarcho, M.P., Leaf, I., Carlson, C.S., Klingensmith, J., Shawlot, W., O'Connor, M.B., 2004. The mammalian twisted gastrulation gene functions in foregut and craniofacial development. Dev. Biol. 267, 374–386.
Petryk, A., Shimmi, O., Jia, X., Carlson, A.E., Tervonen, L., Jarcho, M.P., O'Connor, M.B., Gopalakrishnan, R., 2005. Twisted gastrulation and chordin inhibit differentiation and mineralization in MC3T3-E1 osteoblast-like cells. Bone 36, 617–626.
Qiu, M., Bulfone, A., Ghattas, I., Meneses, J.J., Christensen, L., Sharpe, P.T., Presley, R., Pedersen, R.A., Rubenstein, J.L., 1997. Role of the Dlx homeobox genes in proximodistal patterning of the branchial arches: mutations of Dlx-1, Dlx-2, and Dlx-1 and -2 alter morphogenesis of proximal skeletal and soft tissue structures derived from the first and second arches. Dev. Biol. 185, 165–184.
Roessler, E., Belloni, E., Gaudenz, K., Jay, P., Berta, P., Scherer, S.W., Tsui, L.C., Muenke, M., 1996. Mutations in the human Sonic Hedgehog gene cause holoprosencephaly. Nat. Genet. 14, 357–360.
Ross, J.J., Shimmi, O., Vilmos, P., Petryk, A., Kim, H., Gaudenz, K., Hermanson, S., Ekker, S.C., O'Connor, M.B., Marsh, J.L., 2001. Twisted gastrulation is a conserved extracellular BMP antagonist. Nature 410, 479–483.
Sasaki, H., Hogan, B.L., 1993. Differential expression of multiple fork head related genes during gastrulation and axial pattern formation in the mouse embryo. Development 118, 47–59.
Satokata, I., Maas, R., 1994. Msx1 deficient mice exhibit cleft palate and abnormalities of craniofacial and tooth development. Nat. Genet. 6, 348–356.
Schiffer, C., Tariverdian, G., Schiesser, M., Thomas, M.C., Sergi, C., 2002. Agnathia–otocephaly complex: report of three cases with involvement of two different Carnegie stages. Am. J. Med. Genet. 112, 203–208.
Senders, C.W., Peterson, E.C., Hendrickx, A.G., Cukierski, M.A., 2003. Development of the upper lip. Arch. Facial Plast. Surg. 5, 16–25.
Serpe, M., Umulis, D., Ralston, A., Chen, J., Olson, D.J., Avanesov, A., Othmer, H., O'Connor, M.B., Blair, S.S., 2008. The BMP-binding protein Crossveinless 2 is a short-range, concentration-dependent, biphasic modulator of BMP signaling in *Drosophila*. Dev. Cell 14, 940–953.
Solloway, M.J., Robertson, E.J., 1999. Early embryonic lethality in Bmp5;Bmp7 double mutant mice suggests functional redundancy within the 60A subgroup. Development 126, 1753–1768.
Srinivasan, S., Rashka, K.E., Bier, E., 2002. Creation of a Sog morphogen gradient in the *Drosophila* embryo. Dev. Cell 2, 91–101.
Stottmann, R.W., Anderson, R.M., Klingensmith, J., 2001. The BMP antagonists Chordin and Noggin have essential but redundant roles in mouse mandibular outgrowth. Dev. Biol. 240, 457–473.
Suri, S., Ross, R.B., Tompson, B.D., 2006. Mandibular morphology and growth with and without hypodontia in subjects with Pierre Robin sequence. Am. J. Orthod. Dentofacial. Orthop. 130, 37–46.
Thomas, T., Kurihara, H., Yamagishi, H., Kurihara, Y., Yazaki, Y., Olson, E.N., Srivastava, D., 1998. A signaling cascade involving endothelin-1, dHAND and msx1 regulates development of neural-crest-derived branchial arch mesenchyme. Development 125, 3005–3014.
Tissier-Seta, J.P., Mucchielli, M.L., Mark, M., Mattei, M.G., Goridis, C., Brunet, J.F., 1995. Barx1, a new mouse homeodomain transcription factor expressed in cranio-facial ectomesenchyme and the stomach. Mech. Dev. 51, 3–15.
Tucker, A., Sharpe, P., 2004. The cutting-edge of mammalian development; how the embryo makes teeth. Nat. Rev., Genet. 5, 499–508.
Tucker, A.S., Al Khamis, A., Sharpe, P.T., 1998a. Interactions between Bmp-4 and Msx-1 act to restrict gene expression to odontogenic mesenchyme. Dev. Dyn. 212, 533–539.
Tucker, A.S., Matthews, K.L., Sharpe, P.T., 1998b. Transformation of tooth type induced by inhibition of BMP signaling. Science 282, 1136–1138.
Tucker, J.A., Mintzer, K.A., Mullins, M.C., 2008. The BMP signaling gradient patterns dorsoventral tissues in a temporally progressive manner along the anteroposterior axis. Dev. Cell 14, 108–119.
Vainio, S., Karavanova, I., Jowett, A., Thesleff, I., 1993. Identification of BMP-4 as a signal mediating secondary induction between epithelial and mesenchymal tissues during early tooth development. Cell 75, 45–58.
von der Hardt, S., Bakkers, J., Inbal, A., Carvalho, L., Solnica-Krezel, L., Heisenberg, C.P., Hammerschmidt, M., 2007. The Bmp gradient of the zebrafish gastrula guides migrating lateral cells by regulating cell–cell adhesion. Curr. Biol. 17, 475–487.
Wang, Y.H., Rutherford, B., Upholt, W.B., Mina, M., 1999. Effects of BMP-7 on mouse tooth mesenchyme and chick mandibular mesenchyme. Dev. Dyn. 216, 320–335.
Welsh, I.C., Hagge-Greenberg, A., O'Brien, T.P., 2007. A dosage-dependent role for Spry2 in growth and patterning during palate development. Mech. Dev. 124, 746–761.
Wills, A., Harland, R.M., Khokha, M.K., 2006. Twisted gastrulation is required for forebrain specification and cooperates with Chordin to inhibit BMP signaling during X. tropicalis gastrulation. Dev. Biol. 289, 166–178.
Winnier, G., Blessing, M., Labosky, P.A., Hogan, B.L., 1995. Bone morphogenetic protein-4 is required for mesoderm formation and patterning in the mouse. Genes Dev. 9, 2105–2116.
Zakin, L., Metzinger, C.A., Chang, E.Y., Coffinier, C., De Robertis, E.M., 2008. Development of the vertebral morphogenetic field in the mouse: interactions between Crossveinless-2 and Twisted Gastrulation. Dev. Biol. 323, 6–18.
Zhang, J.L., Qiu, L.Y., Kotzsch, A., Weidauer, S., Patterson, L., Hammerschmidt, M., Sebald, W., Mueller, T.D., 2008. Crystal structure analysis reveals how the Chordin family member crossveinless 2 blocks BMP-2 receptor binding. Dev. Cell 14, 739–750.